

A DECOUPLED PATH-FOLLOWING CONTROL ALGORITHM BASED UPON THE DECOMPOSED TRAJECTORY ERROR

Jia-Yush Yen[†]
Professor,

Hsin-Chiang Ho*
*Senior Engineer

Shu-Shung Lu[†]
Professor

*AFREE Inc., 3F No. 102 Sung Lung Road, Taipei, Taiwan, R.O.C.

[†]Department of Mechanical Engineering, National Taiwan University,
Taipei, Taiwan 10764, R.O.C.
jyen@ccms.ntu.edu.tw

Abstract

This paper proposes a new path-following control algorithm for the machine tool servo systems. The controller first decomposes the normal tracking error from the advancing tangential error. A dynamic decoupling procedure is then proposed to the advancement mechanism and the trajectory tracking mechanism in the machine tool servo. A dynamic decoupling controller is proposed to operate on the decomposed tangential and a normal tracking error. The normal control minimizes the perpendicular tracking error while the tangential control maintains a desired feed rate. The method is applied on an experimental X-Y table, and the results show good tracking and trajectory following characteristics. The new algorithm enables the design of a non-overshooting controller along the path. This would allow no-over-cutting process for the machine tool operation.

1. INTRODUCTION

The machine tool servo systems maintain two control objectives: To follow a pre-specified trajectory as closely as possible, and to maintain a pre-specified advancing speed. The servo systems break the curves into small pieces, and step along these pieces to form the path. When the trajectories are multi-dimensional, the systems divide the motion into simultaneous movements in different axis [1]. The drivers on each axis have to move in synchronous with one another to obtain the desired trajectory. If the controllers operate independently, then any load disturbance or any difference in the performance of each axis may cause contour error [1].

Many researchers have addressed the issue of axis impedance matching [2]-[7]. Sarachik and Ragazzin [2] proposed the "master-slave" structure in 1957 to enhance

the controller's contour follow capability. In 1980, Koren [3] introduced the concepts of *crossed-coupled control* to reduce contour error. Tomizuka, et. al [5][6][7] made different trials to synchronize the two axes motion, and more recently, Kulkarni and Svinivasan [8], [9] formulated the linear-quadratic optimally cross-coupled control problem. There are also efforts based on variable-gain and adaptive control algorithms [10], [11]. The basic concept behind the machine tool control is to eliminate the distance between the cutting tool and the desired surface. However, the formulation for eliminating only this error would result in a standing regulation problem. Thus, all the control algorithms resolve to point-to-point algorithms to achieve motion along the desired path [12], [13], [14]. Previously, different axis has its own controller, which do not obtain the information from other axes [3]. The newer controllers try to overcome this problem by introducing an additional feedback law derived from the path-following error such that the system's contour error rejection capability is enhanced.

In this paper, the authors believe that the contour error represents a *trajectory regulation* problem. A good motion controller should achieve trajectory regulation at any time. On the other hand, the movement along the trajectory represents a *speed regulation* problem. It is thus nature to decouple the control action into a normal control action, which regulates the system around the desired trajectory, and a tangential control action, which manipulates the speed control problem. To achieve this purpose, one has to first decompose the tracking error into a normal and a tangential component. Separated control laws must then be applied to a dynamically decoupled system for independent tracking and feed rate control. Base on this argument, this paper thus proposes a new control algorithm, in which a dynamic decoupling

controller operates on the decomposed error to achieve independent tracking and feed rate control. Experimental results show that the proposed control algorithm achieves a smoother cutting contour and enables a direct treatment on the contour error specifications. This design algorithm allows the design of non-overshooting controller around the curve. In the practice, it provides a way to design of a machine tool servo that does not undergo over cutting problem.

The rest of this paper is organized as follows. Section 2 presents the command generation procedure. Section 3 presents the key dynamic decoupling algorithm. Section 4 offers an illustrative example on the circular curve-tracking problem as well as the experimental setup. Section 5 reveals the experimental results and discussion. Finally, section 6 provides some concluding remarks and directions for future study.

2. REFERENCE COMMANDS GENERATION

As described in the introduction, the desired curve in the machine tool is usually represented in parametric form as $P_d(x(u), y(u), z(u))$, $u \in [0, L]$ (figure 1) [13]. Assume that the position of the tool at some time is at P_i . Because the target is the curve P_d , two separate directions are considered: a normal error and a tangential error. Ideally, the normal controller reduces the contour error; and the tangential controller maintains the desired feed-rate, or cutting speed. Together, they achieve the manufacturing accuracy.

The procedures to define the feedback errors are divided in two parts: 1) define the projection point P_d and find the contour error e_c , and 2) define the target point for the next step P_{d+i} along the desired curve according to the specified acceleration or feed-rate;

2.1 Finding the contour error e_c

Given a parametric curve that is represented as $P_d(x(u), y(u), z(u))$, where $u \in [0, L]$. The tangential vector is defined by $t = dP_d / du$. Assuming that the projection of a point in the 3D space, say $P_i(x_i, y_i, z_i)$, to this curve is $P_{di}(x(u_i), y(u_i), z(u_i))$, in

which u_i is obtained by solving $(P_{di} - P_i) \cdot t = 0$. Then, the contour error is the distance between P_i and P_{di} .

$$|e_c| = |P_{di} - P_i| = \sqrt{(x(u_i) - x_i)^2 + (y(u_i) - y_i)^2 + (z(u_i) - z_i)^2} \quad (1)$$

2.2 The on-line interpolator

Consider the same curve as in figure 1, and allow $V(u)$ to be the desired velocity vector along this curve. $V(u)$ is defined by

$$V(u) = \frac{dP_d}{dt} = \frac{dP_d}{du} \frac{du}{dt} = \left(\frac{dx}{du} \bar{i} + \frac{dy}{du} \bar{j} + \frac{dz}{du} \bar{k} \right) \frac{du}{dt} \quad (2)$$

$$|V(u)| = \left| \frac{dP_d}{du} \right| \frac{du}{dt} \quad (3)$$

Assume that one specifies the acceleration $|A(u)|$, which is defined by

$$|A(u)| = \frac{d|V(u)|}{dt} = \frac{d|V(u)|}{du} \frac{du}{dt} \quad (4)$$

From (3)

$$|A(u)| = \frac{d|V(u)|}{du} \frac{|V(u)|}{|dP_d / du|} \quad (5)$$

Hence,

$$\int_{u_0}^u |A(u')| \left| \frac{dP_d}{du'} \right| du')^{1/2} = \int_{V(u_0)}^{V(u)} |V(u')| d|V(u')|. \quad (6)$$

According to Huang and Yang [7],

$$|V(u)| = \left[|V^2(u_0)| + 2 \int_{u_0}^u |A(u')| \left| \frac{dP_d}{du'} \right| du' \right]^{1/2} \quad (7)$$

From equation (3) we have

$$\int_{u_0}^u \frac{|dP_d / du|}{|V(u')|} du = \int_{t_0}^t dt \quad (8)$$

Combine equations (7) and (8), and let $u_0 = u_i$, $u = u_{i+1}$, $t_0 = t_i$, $t = t_{i+1}$, P_{d+i+1} can be obtained.

Then the reference inputs at the time t_{i+1} is set to $P_{di+1} - P_i$.

3. DECOUPLED DYNAMICS

After getting the normal feedback signal and the feed rate reference point, one needs to find the system structure to carry out separate normal and tangential controller design. Consider for example a x-y table, the dynamics of x and y-axes are $g_{11}(s)$ and $g_{22}(s)$, respectively, i.e.

$$\begin{bmatrix} y_x(s) \\ y_y(s) \end{bmatrix} = \begin{bmatrix} g_{11}(s) & 0 \\ 0 & g_{22}(s) \end{bmatrix} \begin{bmatrix} u_x(s) \\ u_y(s) \end{bmatrix} = \mathbf{G}(s) \begin{bmatrix} u_x(s) \\ u_y(s) \end{bmatrix} \quad (9)$$

To obtain the dynamics in the tangential and the normal directions to the desired trajectory, one proceeds by defining a transformation matrix, \mathbf{F} , between the errors in the x, y directions, e_x and e_y , and the errors in the tangential and normal directions, e_t and e_n . (As shown in figure 2.) Thus \mathbf{F} can be expressed as

$$\mathbf{F} = \begin{bmatrix} f_{11} & f_{12} \\ f_{21} & f_{22} \end{bmatrix} = \begin{bmatrix} \cos\theta & \sin\theta \\ -\sin\theta & \cos\theta \end{bmatrix}, \quad (10)$$

where θ is the angle between the x-axis and the tangent of the desired trajectory. Therefore,

$$\begin{bmatrix} y_t(s) \\ y_n(s) \end{bmatrix} = \mathbf{F} \begin{bmatrix} y_x(s) \\ y_y(s) \end{bmatrix} = \mathbf{F} * \mathbf{G} \begin{bmatrix} u_x(s) \\ u_y(s) \end{bmatrix}. \quad (11)$$

In order to decouple the system dynamics into tangential and normal directions, define a de-coupling matrix which acts like a filter between $\begin{bmatrix} u_t(s) \\ u_n(s) \end{bmatrix}$ and $\begin{bmatrix} u_x(s) \\ u_y(s) \end{bmatrix}$, i.e.

$$\begin{bmatrix} u_x(s) \\ u_y(s) \end{bmatrix} = \begin{bmatrix} C_{11}(s) & C_{12}(s) \\ C_{21}(s) & C_{22}(s) \end{bmatrix} \begin{bmatrix} u_t(s) \\ u_n(s) \end{bmatrix} = \mathbf{C} \begin{bmatrix} u_t(s) \\ u_n(s) \end{bmatrix} \quad (12)$$

Substitute (10) into (9)

$$\begin{bmatrix} y_t(s) \\ y_n(s) \end{bmatrix} = \mathbf{F} \mathbf{G} \mathbf{C} \begin{bmatrix} u_t(s) \\ u_n(s) \end{bmatrix} = \mathbf{G}_t \begin{bmatrix} u_t(s) \\ u_n(s) \end{bmatrix} \quad (13)$$

If there exists a \mathbf{C} that diagonalizes \mathbf{G}_t , then the system dynamics can be decoupled into

$$\mathbf{G}_t(s) = \begin{bmatrix} g_{t_{11}}(s) & 0 \\ 0 & g_{t_{22}}(s) \end{bmatrix}.$$

From (11),

$$\begin{bmatrix} g_{t_{11}} & 0 \\ 0 & g_{t_{22}} \end{bmatrix} = \begin{bmatrix} c_{11} & c_{12} \\ c_{21} & c_{22} \end{bmatrix} \begin{bmatrix} f_{11} & f_{12} \\ f_{21} & f_{22} \end{bmatrix} \begin{bmatrix} g_{11} & 0 \\ 0 & g_{22} \end{bmatrix} \\ = \begin{bmatrix} c_{11} & c_{12} \\ c_{21} & c_{22} \end{bmatrix} \begin{bmatrix} f_{11}g_{11} & f_{12}g_{22} \\ f_{21}g_{11} & f_{22}g_{22} \end{bmatrix},$$

or,

$$\begin{cases} g_{t_{11}} = c_{11}f_{11}g_{11} + c_{12}f_{21}g_{11} \\ 0 = c_{11}f_{12}g_{22} + c_{12}f_{22}g_{22} \\ 0 = c_{21}f_{11}g_{11} + c_{22}f_{21}g_{11} \\ g_{t_{22}} = c_{21}f_{12}g_{22} + c_{22}f_{22}g_{22} \end{cases} \quad (14)$$

Solving (14), we get

$$\mathbf{C} = \begin{bmatrix} -\frac{f_{22}}{(f_{11}f_{22} - f_{12}f_{21})} \frac{g_{t_{11}}}{g_{11}} & -\frac{f_{12}}{(f_{11}f_{22} - f_{12}f_{21})} \frac{g_{t_{22}}}{g_{22}} \\ -\frac{f_{21}}{(f_{11}f_{22} - f_{12}f_{21})} \frac{g_{t_{11}}}{g_{11}} & \frac{f_{11}}{(f_{11}f_{22} - f_{12}f_{21})} \frac{g_{t_{22}}}{g_{22}} \end{bmatrix} \quad (15)$$

\mathbf{C} must satisfy some constraints:

- 1) \mathbf{C} must be stable to avoid internally unstable. Therefore,
 - $g_{t_{11}}$ must have stable poles.
 - $g_{t_{11}}$ must contain all the non-minimal phase zeros of g_{11} 's.
 - $g_{t_{22}}$ must have stable poles.
 - $g_{t_{22}}$ must contain all the non-minimal phase zeros of g_{22} 's.
- 2) \mathbf{C} must be realizable. Therefore,
 - The relative degrees of $g_{t_{11}}$ must be greater than the relative degrees of g_{11} .
 - The relative degrees of $g_{t_{22}}$ must be greater than the relative degrees of g_{22} .

From (15), one obtains a dynamically decoupled system in the form of (13), whose dynamics are decoupled into a tangential and a normal (contouring) directions according to the desired contour. The block diagram for system design thus becomes as shown in figure 3. With this setup, conceptually, the decoupled controller, $\bar{\mathbf{K}}(s)$, design can be carried out in the tangential and normal directions. The actual controller to be implemented is $\mathbf{K}(s)$ in the figure.

4. Experiment Setup and Test Example

Figure 4 presents the experiment X-Y table. The table is 850Kg in weight and the strokes of X and Y-axes are 400mm and 300mm. The measurement resolution in both axes is 10 μm . Two AC servomotors each drive a ball-screw to position the X-Y table. The resolvers mounted on the end of the servomotors measure the position of the table. A counter board in the control computer takes the position counts. The control computer, a 486-based PC, calculates the errors and computes the control effort. Because of the friction of this table and the saturation of drive, a filter is also included to compensate for the control input.

As an illustration example, consider a circular path as shown in figure 5. Each point on the path can be represented by

$$P_d(x(u), y(u)) = P_d(r \cos u, r \sin u). \quad (16)$$

The tangent direction at point P_d is

$$t = \frac{dP_d}{du} = (-r \sin u, r \cos u). \quad (17)$$

Follow section 2, we have

$$\begin{aligned} (P_d - P_i) \cdot t &= 0 \\ (r \cos u - x_i, r \sin u - y_i) \cdot (-r \sin u, r \cos u) &= 0 \\ x_i \sin u &= y_i \cos u \\ u_i &= \tan^{-1}\left(\frac{y_i}{x_i}\right) \end{aligned}$$

and

$$P_{di} = (r \cos(\arctan(\frac{y_i}{x_i})), r \sin(\arctan(\frac{y_i}{x_i}))). \quad (18)$$

The contour error in the normal direction is thus,

$$\begin{aligned} |e_c| &= |P_i - P_{di}| \\ &= \sqrt{(x_i - r \cos(\tan^{-1}(\frac{y_i}{x_i})))^2 + (y_i - r \sin(\tan^{-1}(\frac{y_i}{x_i})))^2}. \end{aligned} \quad (19)$$

If we specify the acceleration $|A(u)|$ and the maximum allowable feed-rate F for a trapezoidal velocity profile, then

$$|A(u)| = \begin{cases} A & \forall V(u_{i+1}) < F(\text{Feedrate}) \\ 0 & \forall V(u_{i+1}) \geq F(\text{Feedrate}) \end{cases} \quad (20)$$

$$u_{i+1} = \frac{AT^2}{2} + \frac{TV(u_i)}{r} + u_i, \text{ where } T \text{ is sampling period and}$$

$$V(u_{i+1}) = [V^2(u_i) + 2Ar(u_{i+1} - u_i)]^{1/2} \quad (21)$$

under condition that $V(u_{i+1}) \geq F$,

$$\begin{cases} u_{i+1} = \frac{TF}{r} + u_i \\ V(u_{i+1}) = F \end{cases} \quad (22)$$

Therefore,

$$P_{di+1} = (r \cos(u_{i+1}), r \sin(u_{i+1})). \quad (23)$$

Finally, the reference input is

$$R_{i+1} = P_{di+1} - P_i = (r \cos(u_{i+1}) - x_i, r \sin(u_{i+1}) - y_i) \quad (24)$$

After getting the reference input, can separately design the normal and tangential controllers with traditional design algorithms.

In this example, we use the MATLAB Nonlinear Control Toolbox to find a non-overshoot controller for the nominal control. No overshoot in the normal direction means non-over cutting in the machining process. Because the decoupling is obtained for every position, this controller will achieve no over cutting throughout the trajectory.

5. Results and Discussion

Figures 6~9 summarize the experimental results. In the following figures, figure (a) shows the desired and the actual trajectory. Figure (b) displays the time responses. Figure (c) shows the contour error, and figure (d) shows the control effort. Figure 6 contains the result of the table making a 20 mm circle with cross-coupled control. The feed-rate in this case is set to 20 mm/sec. Figure 7 is the same test condition as figure 6 with a doubled cross-coupled controller gain. It can be seen that the contour error is reduced which matches with the aim of cross-coupled controller. It is noteworthy that the tracking speed increases a little. That is because the cross-coupled control input becomes larger so that the drives move faster not only in contouring direction but also in tangential direction. Further increasing the cross-coupled controller gain to three times (figure 8), we can see that although the contour error decreases a little further but it starts to cause undesirable chattering.

Figure 9 shows the results of the decoupled controller proposed in this paper. The command generate procedure is the same as those in figures 6~8. We see that the contour error is in the range of figure 7 and better than figure 6. Moreover, it is very successful in avoiding over cutting, which was part of the original goal in the normal controller. Actually, because of the non-overshoot criterion, the response is slower than figures 6 and 8.

6. Conclusions

This paper proposed a new path following controller with decoupled tangential and the normal control. The controller de-couples the tracking system into a normal contour error dynamics and a tangential speed regulation dynamics. The normal control is responsible for maintaining the tool on the target trajectory, and the tangential control will move the tool along the trajectory at the desired speed. Since the errors must be calculated on-line, an on-line interpolator is introduced in the controller. This approach makes the new controller more robust system delays because the on-line command generator is not affected by the delay cause by different material hardness or path obstacles. With the advanced computer speed, doing so during each sampling period does not seem to have any drawbacks.

The new decoupled controller can be regarded as a modification to the cross-coupled controller. This approach maintains the advantages of the cross-coupled controller, while clearly identifying the control effort to drive the tool along the desired trajectory. Thus, the new controller allows for a distinct trajectory regulation and feed-rate specifications. The experimental results demonstrated that the decoupled controller is capable of achieving the separate trajectory following and feed rate requirements. In addition, the new controller also achieves non-overshoot control to avoid over cutting.

Acknowledgements

This work was sponsored by the National Science Council, R.O.C. under project No. NSC85-2212-E-002-060.

References

- [1]. Koren, Y., 1979, "Design of Computer Control for Manufacturing Systems," *ASME Journal of Engineering for Industry*, Vol. 101, pp. 326-332.
- [2]. Sarachik, P., and Ragazzini, J. R., 1957, "A Two Dimensional Feedback Control System," *Trans. AIEE*, Vol. 76, Part II, May, pp.55-61
- [3]. Koren, Y., 1980, "Cross-Coupled Biaxial Computer Control for Manufacturing Systems," *ASME Journal of Dynamic Systems, Measurement, and Control*, Dec., Vol. 102, pp.265-272
- [4]. Koren, Y., and Lo, C. C., 1992, "Advanced Controllers for Feed Drives," *Annals of the CIRP*, Vol. 41/2, pp. 686-698.
- [5]. Tsao, T. C. and Tomizuka, M., 1988, "Adaptive Zero Phase Error Tracking Algorithm for Digital Control," *ASME Journal of Dynamic Systems, Measurement and Control*, Vol. 109, pp. 349-354
- [6]. Bulter, J., Haack, B., and Tomizuka, M., 1991, "Reference Generation for High Speed Coordinated Motion of a Two Axis System," *ASME Journal of Dynamic Systems, Measurement and Control*, vol.113, No.1, pp.67-74.
- [7]. Tomizuka, M., Hu, J. S., Chiu, T. C., and Kamano, T., 1992, "Synchronization of Two Motion Control Axes Under Adaptive Feedforward Control," *ASME Journal of*

Dynamic Systems, Measurement and Control, vol.114, pp.196-203.

[8]. Kulkarni, P. K., and Srinivasan, K., 1989, "Optimal Contouring Control of Multi-Axial Feed Drive Servomechanisms," *ASME Journal of Engineering for Industry*, Vol. 111, pp. 140-148.

[9]. Kulkarni, P. K. and Srinivasan, K., 1990, "Cross-Coupled Control of Biaxial Feed Drive Servomechanisms," *ASME Journal of Dynamic Systems, Measurement and Control*, Vol. 112, No. 2, pp. 225-232.

[10]. Koren, Y., and Lo, Ch.-Ch., 1991, "Variable-Gain Cross-Coupling controller for Contour," *Annals of the CIRP*, Vol. 40/1, pp. 371-373.

[11]. Chuang, H. Y. and Liu, C. H., 1991, "Cross-Coupled Adaptive Feedrate Control for Multiaxis Machine Tools," *ASME Journal of Dynamic Systems, Measurement and Control*, Vol. 106, pp. 451-457.

[12]. Masory, O. and Koren, Y., 1982, "Reference Word Circular Interpolators for CNC Systems," *ASME Journal of Engineering for Industry*, Vol. 104, pp. 400-405.

[13]. Hunag, J. T. and Yang, D. C. H., 1992, "Precision command generation for computer controlled machines," *Precision Machining: Technology and Machine Development and Improvement*, PED-Vol.58 ASME.

[14]. Stadelmann, R., 1989, "Computation of Nominal Path Values to Generate Various Special Curves for Machine," *Annals of the CIRP*, Vol.38/1, pp. 373-376

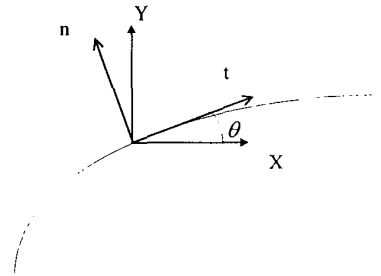


Figure 2 Geometry of XY coordinate and tangential-normal coordinate

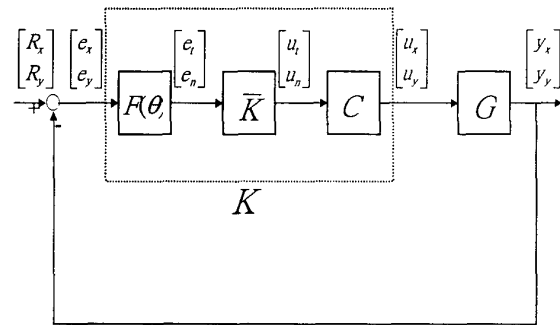


Figure 3 Block diagram of decoupled control structure

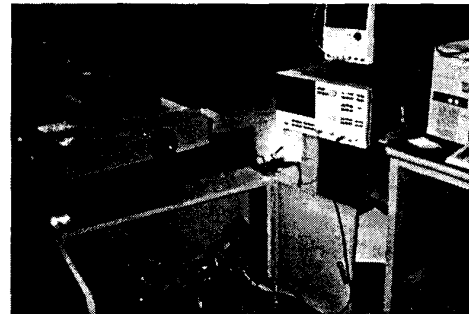


Figure 4 Experiment setup

FIGURES

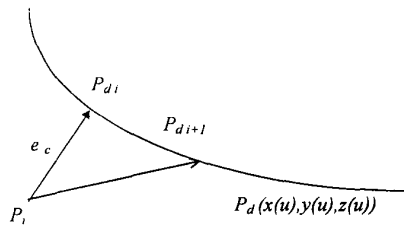


Figure 1 Geometry of the contour error

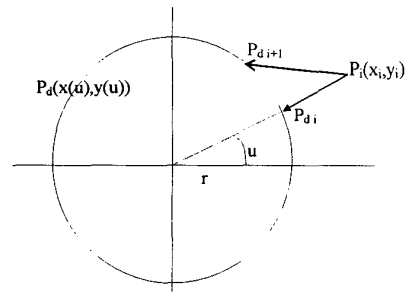


Figure 5 Circular path command generation

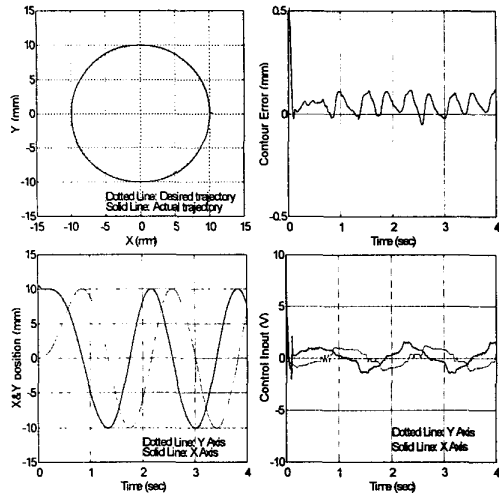


Figure 6 Cross Coupled controller acting with reference feed-rate = 20 mm/s.

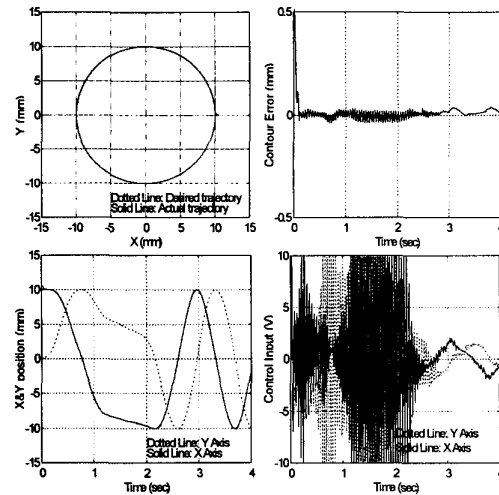


Figure 8 Cross Coupled controller acting with reference feed-rate = 20 mm/s and cross coupled control input gain is tripled

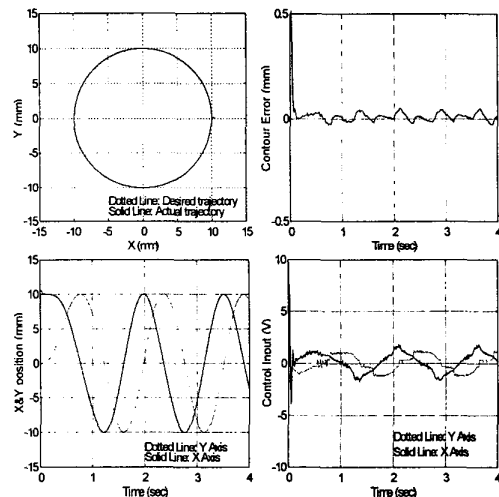


Figure 7 Cross Coupled controller acting with reference feed-rate = 20 mm/s and cross coupled control input gain is doubled

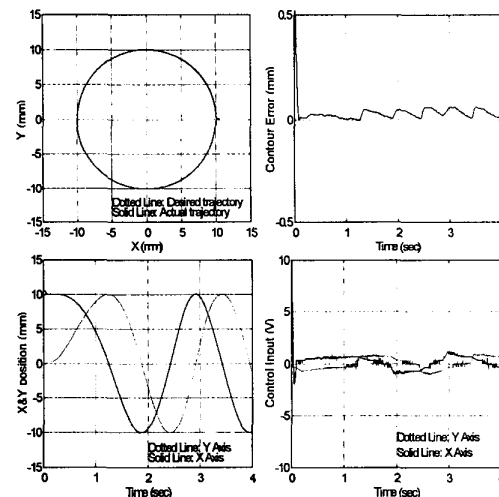


Figure 9 Decoupled controller acting with reference feed-rate = 20 mm/s